

Featuring research from the groups of Professor Hongwen Ren at Chonbuk National University, South Korea and Professor Shin-Tson Wu at the University of Central Florida, USA.

Title: Liquid crystal pump

Through balancing the dielectric force and surface tension, a liquid-crystal droplet can do reciprocating movement. Such a droplet functions as a micropump, which may find attractive applications in adaptive lens, liquid drug delivery, and biotechnology.

As featured in:

Lab on a Chip

Miniaturisation for chemistry, physics, biology, materials science and bioengineering



RSC Publishing

ISSN 1466-7220
http://www.rsc.org/loc



See Ren *et al.*,
Lab Chip, 2013, **13**, 100-105.

RSC Publishing

www.rsc.org/loc

Registered Charity Number 207890

PAPER

Liquid crystal pump†

Hongwen Ren,^{*a} Su Xu^b and Shin-Tson Wu^bCite this: *Lab Chip*, 2013, 13, 100

We report a dielectrically actuated liquid crystal (LC) pump. A small volume of LC forms a pillar-like droplet in a cylindrical hole which partially touches the bottom substrate with embedded interdigitated electrodes. By applying a voltage, the LC droplet can be largely stretched along the electrode direction by the generated dielectric force, which in turn exerts a pressure to displace a small volume of fluid on the opposite side of the chamber. Once the voltage is removed, the LC droplet returns to its initial state. The LC droplet with such a reciprocating movement behaves like a pump. In this work, the actuation mechanism of the LC pump is presented and the performance evaluated experimentally. Our LC pump has the following advantages: simple structure, easy fabrication, compact size, high precision, low power consumption, and relatively fast response time. It is promising for applications in lens actuators, biotechnology, drug delivery, and other lab-on-a-chip devices.

Received 20th August 2012,
Accepted 24th September 2012

DOI: 10.1039/c2lc40953d

www.rsc.org/loc

Introduction

Liquid crystals (LCs) have been widely used in displays,¹ phase modulators,^{2,3} information storage,⁴ optical switches,^{5–9} optical communications,¹⁰ adaptive lenses,^{11–13} and other photonic devices.¹⁴ Although the applications are different, the basic operation principles can be roughly classified into two categories: electric field-induced LC molecular reorientation, and electric field-induced LC shape deformation. The former mechanism has been investigated for decades, but the latter is relatively new and has attracted a lot of research attention recently. Several photonic devices based on dielectrophoresis-induced LC shape deformation have been demonstrated.

Most LCs are preferred dielectric materials because of their high electrical resistivities. In the mesogenic phase, an LC compound presents two principal relative permittivities: $\epsilon_{//}$ (parallel to the director) and ϵ_{\perp} (perpendicular to the director). Dielectric anisotropy is defined as $\Delta\epsilon = \epsilon_{//} - \epsilon_{\perp}$. For a positive LC, $\Delta\epsilon > 0$, and *vice versa*. When a small LC droplet is subject to a non-uniform electric field, the LC molecules at the droplet edge experience two torques: electric torque and dielectric torque. If the dielectric constant of the surrounding medium (air or oil) is smaller than $\epsilon_{//}$, then the LC molecules will be pulled outward. Due to the cohesive force of the adjacent LC molecules, the droplet will expand or spread out. Upon removing the voltage, the droplet will return to its initial

shape due to the interfacial tension. Unlike common liquids, some LCs exhibit a large $\Delta\epsilon$ and medium surface tension. Therefore, under the same operating voltage, a large shape deformation can be obtained.

In our previous reports,^{8,9} shape-deformable LC droplets have been used for beam control, optical switches, and displays. However, these applications are mainly limited to conventional photonic devices. To further extend the applications, there is a desire to develop innovative concepts that can overcome the traditional limit of LC technology.

Besides LCs, the field of microfluidics is also growing rapidly. Useful applications of microfluidics can be found in biology, drug delivery, microelectronics cooling, and lab-on-a-chip systems.^{15–20} One of the most important components of a microfluidic device is a micropump, which provides the driving force to displace a fluid. Several pressure-driven micropumps, based on piezoelectrics, electrostatics, thermopneumatics, shape memory alloy, electrowetting, and electromagnetics have been developed. Among them, the micropumps based on electrowetting¹⁸ and electromagnetics¹⁹ are considered as non-mechanical (no moving solid parts) pumps, so their driving system is compact and easy to handle. However, the electrowetting-based micropump works aperiodically and its device fabrication is rather complicated. On the other hand, the electromagnetics-based micropump presents a perfect reciprocating oscillation for mobilizing a fluid. But power consumption is a concern because it is a current-driven device.

Inspired by the ferrofluidic droplets for pumping fluids,¹⁹ here we report a pillar-like droplet which can function as a pump. In an airtight chamber, an LC droplet with a reciprocating movement exerts a pressure to a small volume of fluid, which leads to a displacement of the fluid. The fast-

^aDepartment of Polymer Nano Science and Technology, Chonbuk National University, Jeonju, Jeonbuk, South Korea. E-mail: hongwen@jbnu.ac.kr; Fax: +82-63-270-2341; Tel: +82-63-270-2354

^bCollege of Optics and Photonics, University of Central Florida, Orlando, USA. E-mail: suxu@creol.ucf.edu; swu@mail.ucf.edu; Fax: +1 407-823-6880; Tel: +1 407-823-4763

† Electronic supplementary information (ESI) available: Supplementary movies. See DOI: 10.1039/c2lc40953d

response reciprocating oscillation makes our LC pump a key component in microfluidic devices. It exhibits the following advantages over the previous fluid pumps: easy fabrication, voltage driven, precise control, and low power consumption. This work opens a new gateway for extending the applications of LCs to microfluidic devices.

Actuation mechanism

Device structure

Unlike a macroscale liquid droplet, surface tension of micro- and nano-scale liquid droplets is dominant over the body forces, such as gravity or inertia. Therefore, such a liquid droplet can maintain a spherical surface in air. If the droplet is deformed by an external force, and once the force is removed, the surface tension plays an important role in the liquid recovery. Our new concept of using an LC droplet to pump a fluid is illustrated in Fig. 1. The chamber consists of two glass substrates, which are separated by spacers. The top substrate has two drilled holes, one for the LC droplet and one for the fluid droplet. A small LC droplet is filled in the right hole, which touches the bottom substrate. This LC droplet forms a pillar-like shape in the hole. Another small volume of fluid is dripped in the left hole. When the whole system reaches an equilibrium state, the fluid droplet suspends in the left hole, partially contacting with the top substrate surface, as shown in Fig. 1a. The volume of both droplets can be controlled

according to different applications. The chamber is airtight and its rest space can be filled with a fluid or air. Both surfaces of the top substrate and the inner surface of the bottom substrate are coated with hydrophobic material. As a result, both droplets present a spherical shape on the top substrate surface.

Actuation method

To generate a dielectric force, a gradient electric field is required.^{21,22} Usually a fringing field is preferred to drive the LC droplet, since the operating voltage is insensitive to the droplet size and cell gap. To generate a fringing field, we used interdigitated ITO electrodes, as Fig. 1b shows.

Without an external voltage, the LC droplet presents minimal surface-to-volume ratio. When a voltage is applied across the ITO stripes (through terminals A and B), the region between the ITO stripes, but close to the substrate surface, exhibits the highest electric field, and that part of the LC droplet (close to the bottom substrate) bears the highest dielectric force along the ITO strip direction.⁸ As a result, it is expanded outward, pulling an extra volume of LC to enter the chamber. Let us assume the volume of the air in the chamber is incompressible, then the LC droplet exerts a pressure to the fluid droplet, causing the fluid droplet to move upward, as depicted in Fig. 1c.

When the voltage is removed, the deformed LC droplet recovers to its original state because of surface tension, and the fluid droplet returns to its initial position accordingly. By cyclically oscillating the LC droplet, the fluid droplet can perform reciprocating movement in the left hole.

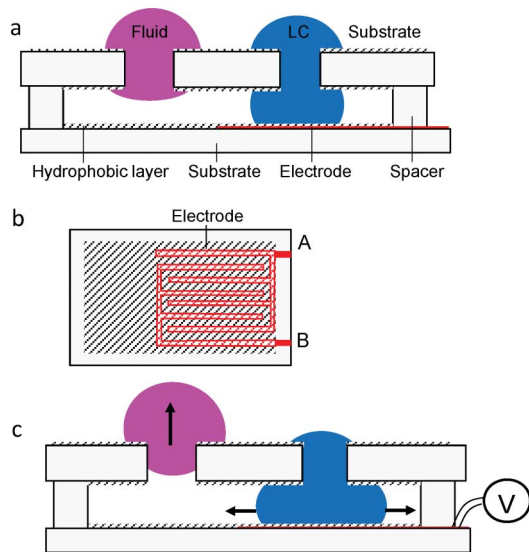


Fig. 1 **a**, Side view of the device structure. An LC droplet filled in the right hole partially contacts with the bottom substrate. A fluid droplet is floating in the left hole. The two droplets are separated by a certain distance in order to avoid crosstalk. The cell gap is controlled by spacers and the chamber is tightly sealed. **b**, Layout of the bottom substrate. The inner surface of the bottom substrate is coated with interdigitated indium tin oxide (ITO) electrodes (marked as red), on the top of which is a hydrophobic layer (marked as hatched). **c**, When an additional volume of LC is pulled into the chamber by the generated dielectric force, the left fluid droplet shifts upward. The hole size, cell gap, and width of the ITO strip are not drawn to scale.

Device fabrication

To fabricate the device shown in Fig. 1(a), we first etched the ITO electrode on the bottom substrate. The electrode width and gap are 10 μm and 10 μm , respectively. To increase actuation power (the ability to pump the volume of a fluid), we drilled three holes on the top substrate (thickness ~ 1.7 mm): two for LC pumps and one for the fluid droplet. The diameter of each hole is ~ 2 mm. The two holes for the LC droplets are separated by ~ 6 mm, and they are further separated by ~ 8 mm from the hole for the fluid droplet. Next, we coated Teflon (AF1600) as the hydrophobic layer on the inner surface of the bottom substrate and both surfaces of the top substrate. The formed substrate surface presents a very low surface tension at room temperature. The two substrates formed a cell (or a chamber), and the cell gap was controlled to be ~ 0.7 mm using glass spacers. The periphery of the cell was tightly sealed by glue.

Here we chose a commercial LC mixture ZLI-4389 (Merck, $\epsilon_{11} = 56$, $\Delta\epsilon = 45.6$, $\gamma \sim 35$ mN m $^{-1}$, and $\rho \sim 0.98$ g cm $^{-3}$) as the LC droplet material, which exhibits a high dielectric constant but a medium surface tension in comparison with conventional LCs. Therefore, such an LC droplet can be easily pulled into the chamber and then largely stretched by a relative low voltage.^{8,21} Otherwise, the droplet deformation will be very limited even under a very high voltage. For easy observation,

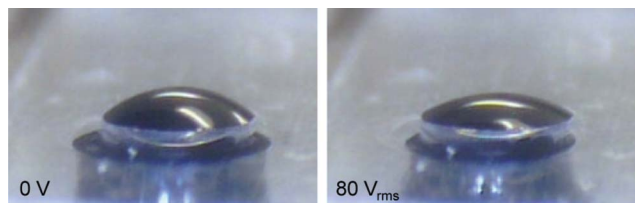


Fig. 2 The shape change of an LC droplet dome at $V = 0$ (left) and $V = 80 V_{\text{rms}}$ (right). The diameter of the hole is 2 mm. The LC droplet is doped with 0.2 wt% black dye and the rest space of the chamber is filled with air. A video of dynamically shifting the droplet dome is also provided in the ESI.†

we doped the LC with ~ 0.2 wt% black dye (S-428, from Mitsui Fine Chemicals). The two holes were filled with the same volume of LC. A small volume of glycerol ($\sim 3.9 \text{ mm}^3$) was dripped in the third hole. The filled LC and glycerol droplets exhibit the smallest surface-to-volume ratio. In our experiments, the rest space of the chamber was filled with air.

Actuation and dynamic response

The dynamic actuation of the LC pump was recorded using a digital CCD camera. Fig. 2 shows the shape change of the droplet dome at voltage-off and voltage-on states. At $V = 0$, the pillar dome has a circular contact area with an aperture of ~ 2 mm. The apex distance of the droplet is ~ 0.7 mm. The droplet presents the smallest surface-to-volume ratio. When the voltage is increased to $40 V_{\text{rms}}$, the droplet begins to sink. At $V = 80 V_{\text{rms}}$, the deformation becomes more noticeable. Further sinking goes on if the voltage continues to increase. Upon removing the voltage, the droplet returns to its original position as well as the initial shape due to surface tension, although the gravity effect is not negligible here. Fig. 3 shows the volume of the LC pulled into the chamber at various voltages. As the voltage increases, the volume of the LC pulled into the chamber is increased accordingly. Because the volume of the chamber is fixed, the glycerol droplet experiences a pressure. As a result, it is pushed upward.

Fig. 4 shows the side view of the glycerol droplet in the voltage-off state. Two LC pumps (blurry) behind the droplet are

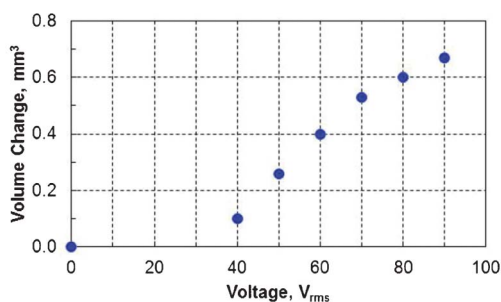


Fig. 3 Additional volume of an LC droplet pulled into the chamber at different voltages.

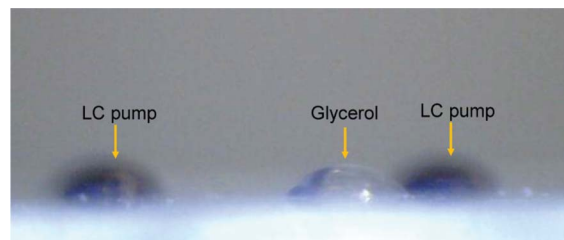


Fig. 4 The dome of the glycerol droplet (aperture ~ 2 mm) in the voltage-off state. To dynamically observe the reciprocating movement of the droplet and two LC pumps, a video is provided in the ESI.†

also included in Fig. 4. The dynamic shape change of the glycerol is recorded in a video. From the video, as the LC pumps are pulled down the glycerol droplet is pushed up. They have reciprocating movement but in an opposite phase.

To evaluate the impact of the LC pumps on the glycerol droplet, a simple way is to measure the light modulation of the oscillated glycerol droplet. Fig. 5a depicts the experimental setup. The cell (only the glycerol droplet is shown) is placed in the horizontal position and a He-Ne laser beam ($\lambda = 633 \text{ nm}$) is normally incident on the glycerol droplet. Due to the bi-convex shape of the droplet, the light passing through the droplet is converged. An iris diaphragm is placed at the focal plane. The transmitted light intensity is detected by a photodiode. A computer controlled LabVIEW data acquisition system was used to drive the cell. At $V = 0$ (solid line), all the incident light is transmitted. At $V = V_1$ (dashed lines), the droplet shifts upward and some light is blocked due to focal length change. Fig. 5b depicts the measured voltage-dependent transmittance change. In the low voltage region, transmittance change is negligible. Above $45 V_{\text{rms}}$, transmittance decreases noticeably, because the droplet is largely deformed and most of the light is blocked by the diaphragm.

For a single LC droplet (pump) shown in Fig. 2, the threshold depends on the exerted dielectric force and the interfacial tensions along the three-phase contact line (solid-LC-air), which can be reduced by employing narrower-gap stripe electrodes, a smaller LC droplet or thinner Teflon layer. While for the glycerol droplet actuated by the LC pumps, only

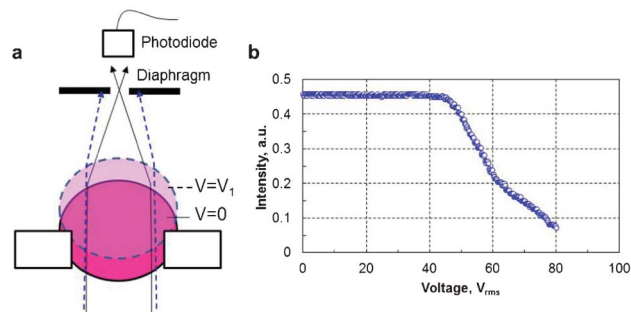


Fig. 5 a. Experimental setup for measuring the light modulation of the actuated glycerol droplet. **b.** Measured light intensity through the glycerol droplet when a variable voltage is applied to the LC pumps.

when the exerted pressure is large enough to overcome the interfacial tensions along the three-phase contact line (solid-glycerol-air), can the glycerol droplet be actuated and the corresponding transmittance decreases. Here the threshold of glycerol actuation is $\sim 45 V_{\text{rms}}$, which is slightly higher than that of the LC volume change ($\sim 40 V_{\text{rms}}$ from Fig. 3). Because when the LC droplet is pulled into the chamber, the air is compressed. The volume of the pulled-in LC is somewhat offset by the air compression in the chamber. Such a discrepancy can be further reduced by replacing the air with a denser gas or incompressible liquid. These two thresholds can also be reduced by lowering the interfacial tension along the three-phase contact line through certain surface treatment.

Because the glycerol droplet can do reciprocating movement, the response time is an important parameter. The dynamic response can be measured by monitoring the time-dependent light intensity change. A digital oscilloscope was connected to the photodiode (shown in Fig. 5a) for displaying the detected light intensity change. Fig. 6 shows the measured time-dependent light intensity change with a 60 V square-wave voltage (500 Hz) applied to the cell. The cycle driving with two periods shows that the dynamic response of the oscillated droplet repeats very well. It takes ~ 160 ms for the glycerol droplet to move to the highest position and ~ 120 ms to return to its original position. Increasing the applied voltage leads to a longer response time. For example, if the voltage is increased to $80 V_{\text{rms}}$, then the glycerol droplet will take ~ 200 ms to reach the highest position and ~ 140 ms to return. This is because the glycerol droplet travels a longer distance to reach the highest position under a higher operating voltage, therefore, the response time gets longer.

Potential applications

An LC-based miniature pump has the advantages of compactness, direct voltage actuation, and fast response time. It can be used to pump very small and precise volumes of liquid. LC pumps with such performances may find numerous applications in optical switches, liquid oscillators, microfluidic systems, biotechnology, drug delivery systems, and other lab-on-a-chip devices. From Fig. 4, the isotropic fluidic (glycerol)

droplet behaves like a lens, so an attractive application of the LC pump is to actuate a liquid lens.

The LC itself can be used as an adaptive lens, but such a lens is polarization dependent because of the birefringence effect of the LC material. A fluidic droplet based on electrowetting,^{23–25} dielectrophoretic effect,^{22,26,27} or thermal effect²⁸ can also function as an adaptive lens, but the shape deformation is rather limited, or the switching speed is quite slow. By using our approach, it is possible to significantly actuate a large-aperture liquid lens by increasing the number of the pumps. The lens performance of the actuated glycerol droplet can be evaluated conveniently using an optical microscope. A resolution target was placed under the droplet. By adjusting the position of the cell in the vertical direction, a clear image can be observed, as shown in Fig. 7. At the rest state, the lens could resolve group 3 and element 5 and the corresponding resolution is $\sim 13 \text{ lp mm}^{-1}$. The resolution is highly dependent on the quality of the drilled hole, the hydrophobic layer as well as the deformed droplet shape. At $V = 0$, back focal distance (BFD) of the droplet was measured to be ~ 5.1 mm. At $V = 80 V_{\text{rms}}$, the BFD was shortened to ~ 4.3 mm. This is because the droplet contracts more as the voltage increases.

For practical applications, the gravity effect of the LC pump and fluid droplet should be considered when the device is placed in a vertical position. To minimize the gravity-induced image distortion, we could surround the LC and fluidic droplets with an immiscible liquid by constructing a two-chamber system and finding density-matched liquids (fluid medium, fluid droplet and LC).

As an important component of a microfluidic device, it is preferred for LC to pump a fluid, *i.e.* the pressure force is conducted by a liquid rather than air. Therefore, in our next experiment we replaced the glycerol droplet with silicone oil ($\epsilon \sim 4.5$) as the medium to fill the chamber and the left hole (Fig. 8a). The silicone oil and LC are immiscible and their densities ($\sim 0.9 \text{ g mm}^{-3}$) match reasonably well.

Similar to the device shown in Fig. 1c, when a voltage is applied across the ITO stripes the LC droplets are pulled down, which in turn pushes the silicone oil to overflow through the left hole. Because of its low surface tension, the silicone oil (blurry image) droplet on the top substrate surface is not

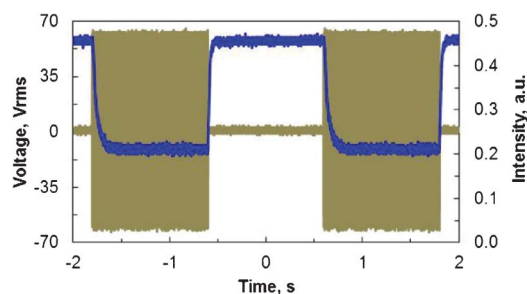


Fig. 6 Measured time-dependent light intensity change. The amplitude of the voltage pulse applied to the LC pump is $60 V_{\text{rms}}$.

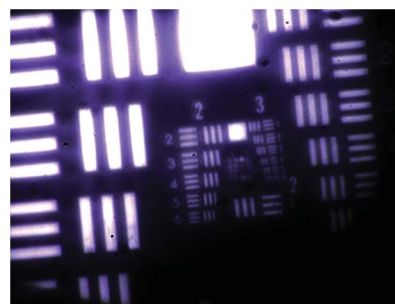


Fig. 7 Measured resolution of the liquid lens (glycerol droplet) under a microscope.

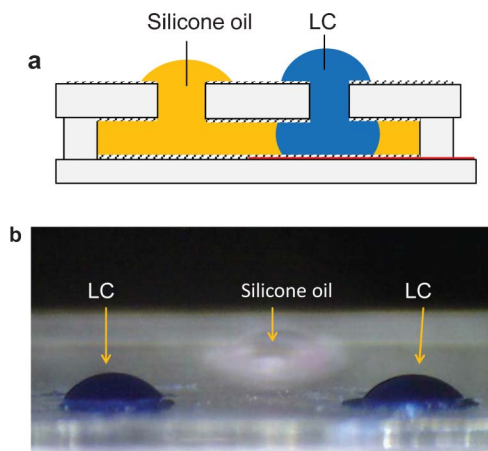


Fig. 8 Two LC droplets for pumping silicone oil. **a**, Side view of the cell structure (the other LC droplet is not shown here). **b**, The rest state of these two LC pumps and silicone oil. A video is provided in the ESI.†

exactly spherical. The response time was measured to be ~ 230 ms for pushing the silicone oil droplet to the highest position and ~ 180 ms for the recovery. By connecting the cell to a refillable fluid reservoir, a continuous displacement (or dispense) of fluids can be achieved, as shown in Fig. 9(a). Here the dome of the LC droplet is covered by a thin elastic membrane to hold the dome of the LC droplet and prevent it from contamination. When a voltage is applied to the cell, the LC droplet is pulled into the chamber and a small amount of liquid is pumped out through the nozzle (Fig. 9(b)). By monitoring the applied voltage, the volume of the pumped liquid can be precisely controlled. Upon removing the voltage, the LC droplet recovers to its original state (Fig. 9(a)). The liquid refilling from the reservoir and the reciprocating movement of the LC droplet enables a continuous and precise liquid (or drug) delivery. If the liquid is miscible with the LC droplet, they can be simply separated by an air slug or a third liquid which is immiscible with them.

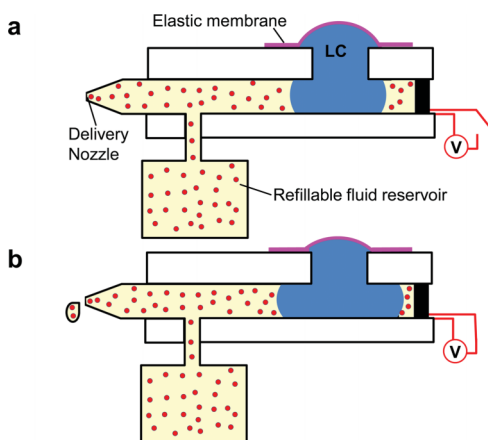


Fig. 9 System for continuous liquid delivery. (a) LC droplet is in contracted state and (b) LC droplet is in stretched state and liquid is dispensed.

From the above experimental results, an LC droplet can function as a pump which provides pressure to a fluid. To increase the pumping power, one approach is to increase the piston number rather than the operating voltage. Due to the direct voltage actuation, the device has the advantages of easy fabrication, compact size, and fast response time. Although the demonstrated LC pump is in the macroscale (aperture ~ 2 mm), it still shows a good reciprocating movement. As we mentioned above, if the LC pump is fabricated on the microscale, then the surface tension will dominate over the gravity force and the device will present a good mechanical stability without the concern of shaking or vibration.

In this work, the employed LC mixture (ZLI-4389) plays an important role. In comparison with common liquids, this LC has a large dielectric constant and high electric resistivity but a medium surface tension, so the shape of the droplet can be largely stretched under a relatively low voltage. In our device, each LC droplet functions as a pump and a group of these LC droplets can actuate a large-aperture fluid droplet. However, the current device structure is by no means optimized. The aperture of holes, thickness of top substrate, cell gap, as well as ITO patterns all need to be optimized in order to enhance the LC pumping power while reducing the actuation voltage.

Conclusion

Based on the surface stretching of a pillar-like LC droplet, we have developed an innovative actuator: LC pump. In a chamber with a two-hole system, if an LC pump in one hole is pulled down by the dielectric force, then a fluid droplet in the other hole is pushed up, because the LC pump provides a pressure to the medium in the chamber, which further propagates to the fluid. The dielectric force is introduced by a fringing field which is generated by the interdigitated electrodes on the bottom substrate. Upon removing the dielectric force, the surface tension of the LC pump pulls the stretched droplet back. Our LC pumps can do reciprocating movement and precisely displace a small volume of fluid. To enhance the pumping power without significantly increasing the actuation voltage, a simple approach is to increase the pump number. The gravity effect can be minimized by using another liquid to balance the gravity of the LC pump and the fluid droplet. Compared to other pumps, our LC pump has the following advantages: simple fabrication, easy actuation, fast response time, and low power consumption. Its potential applications include adaptive photonic devices, microfluidic systems, biotechnology, and other lab-on-a-chip devices.

To dynamically observe the device operation, three videos are available as ESI.†

Acknowledgements

H. Ren is supported by the National Research Foundation of Korea, the international joint research program under grant 20120004814 for the financial support. The University of

Central Florida group is indebted to the U.S. Air Force Office of Scientific Research (AFOSR) for partial financial support under contract No. FA95550-09-1-0170.

References

- 1 M. Schadt and W. Helfrich, *Appl. Phys. Lett.*, 1971, **18**, 127–129.
- 2 D. P. Resler, D. S. Hobbs, R. C. Sharp, L. J. Friedman and T. A. Dorschner, *Opt. Lett.*, 1996, **21**, 689–691.
- 3 T. J. Bunning, S. M. Kirkpatrick, L. V. Natarajan, V. P. Tondiglia and D. W. Tomlin, *Chem. Mater.*, 2000, **12**, 2842–2844.
- 4 V. P. Tondiglia, L. V. Natarajan, R. L. Sutherland, T. J. Bunning and W. W. Adams, *Opt. Lett.*, 1995, **20**, 1325–1327.
- 5 P. S. Drzaic, *J. Appl. Phys.*, 1986, **60**, 2142–2148.
- 6 D. K. Yang, L. C. Chien and J. W. Doane, *Appl. Phys. Lett.*, 1992, **60**, 3102–3104.
- 7 R. A. M. Hikmet and H. J. Boots, *Phys. Rev. E*, 1995, **51**, 5824–5831.
- 8 H. Ren, S. Xu and S. T. Wu, *Lab Chip*, 2011, **11**, 3426–3430.
- 9 S. Xu, H. Ren, Y. Liu and S. T. Wu, *J. Disp. Technol.*, 2012, **8**, 336–340.
- 10 N. A. Riza and S. A. Khan, *Appl. Opt.*, 2004, **43**, 3449–3455.
- 11 S. Sato, *Jpn. J. Appl. Phys.*, 1979, **18**, 1679–1684.
- 12 H. Ren, D. W. Fox, B. Wu and S. T. Wu, *Opt. Express*, 2007, **15**, 11328–11335.
- 13 Y-H. Lin, H.-S. Chen, H.-C. Lin, Y.-S. Tsou, H.-K. Hsu and W.-Y. Li, *Appl. Phys. Lett.*, 2010, **96**, 113505.
- 14 M. Stalder and M. Schadt, *Opt. Lett.*, 1996, **21**, 1948–1950.
- 15 D. Laser and J. G. Santiago, *J. Micromech. Microeng.*, 2004, **14**, 35–64.
- 16 I. Ederer, P. Raetsch, W. Schullerus, C. Tille and U. Zech, *Sens. Actuators, A*, 1997, **62**, 752–755.
- 17 P. Woias, *Sens. Actuators, B*, 2005, **105**, 28–38.
- 18 M. G. Pollack, A. D. Shenderov and R. B. Fair, *Lab Chip*, 2002, **2**, 96–101.
- 19 B. A. Malouin Jr, M. J. Vogel, J. D. Olles, L. Cheng and A. H. Hirs, *Lab Chip*, 2011, **11**, 393–397.
- 20 S. K. Y. Tang, C. A. Stan and G. M. Whitesides, *Lab Chip*, 2008, **8**, 395–401.
- 21 P. Penfield and H. A. Haus, *Electrodynamics of Moving Media*, MIT, Cambridge, 1967.
- 22 C.-C. Cheng, C. Alex and Y. J. Andrew, *Opt. Express*, 2006, **14**, 4101–4106.
- 23 B. Berge and J. Peseux, *Eur. Phys. J. E*, 2000, **3**, 159–163.
- 24 S. Kuiper and H. W. Hendriks, *Appl. Phys. Lett.*, 2004, **85**, 1128–1130.
- 25 S. Grilli, L. Miccio, V. Vespini, A. Finizio, S. De Nicola and P. Ferraro, *Opt. Express*, 2008, **16**, 8084–8093.
- 26 H. Ren, H. Xianyu, S. Xu and S. T. Wu, *Opt. Express*, 2008, **16**, 14954–14960.
- 27 C. C. Yang, C. W. G. Tsai and J. A. Yeh, *J. Microelectromech. Syst.*, 2011, **20**, 1143–1149.
- 28 L. Dong, A. K. Agarwal, D. J. Beebe and H. Jiang, *Nature*, 2006, **442**, 551–554.